Electronic Supplementary Material (ESI) for Physical Chemistry Chemical Physics

Support Information

Octahedral Tin Dioxide Nanocrystals as High Capacity Anode Materials for Na-ion Batteries

Dawei Su[a], Chengyin Wang[b], Hyojun Ahn[c] and Guoxiu Wang*[a]

Received (in XXX, XXX) Xth XXXXXXXXX 20XX, Accepted Xth XXXXXXXXX 20XX

DOI: 10.1039/b000000x

[a] *Centre for Clean Energy Technology, School of Chemistry and Forensic Science, Faculty of Science, University of Technology, Sydney, Australia.*

[b] *College of Chemistry and Chemical Engineering, Yangzhou University, 180 Si-Wang-Ting Road, Yangzhou 225002, China*

[c] *School of Materials Science and Engineering, Gyeongsang National University, Jinju, Gyeongnam 660-701, Republic of Korea*

**Fax: 61-2-9514 1460; Tel: 61-2-9514 1741; E-mail: Guoxiu.Wang@uts.edu.au*

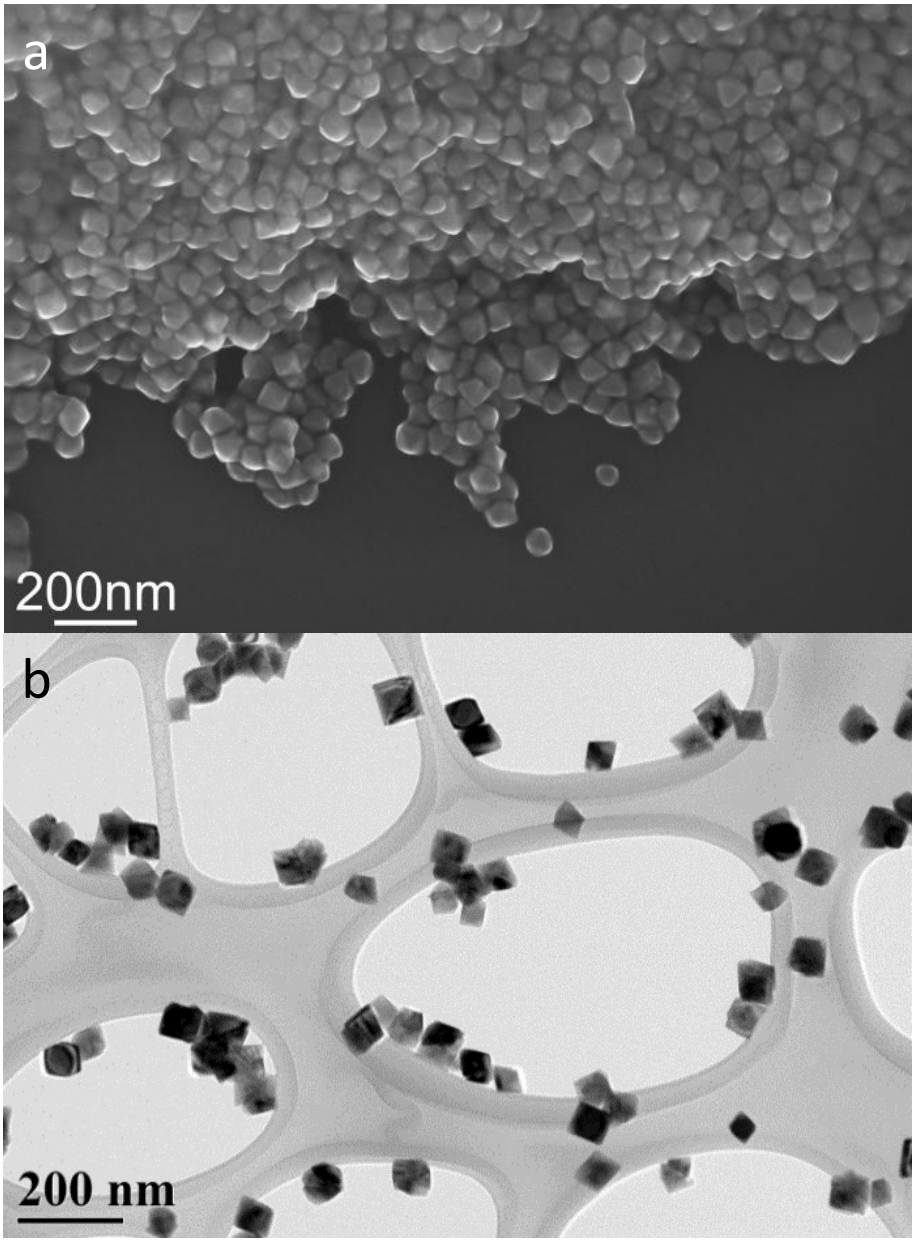

Figure S1. Low magnification FESEM image (a) and TEM image (b) of as-prepared octahedral SnO_2 nanocrystals, showing the homogenous size distribution.

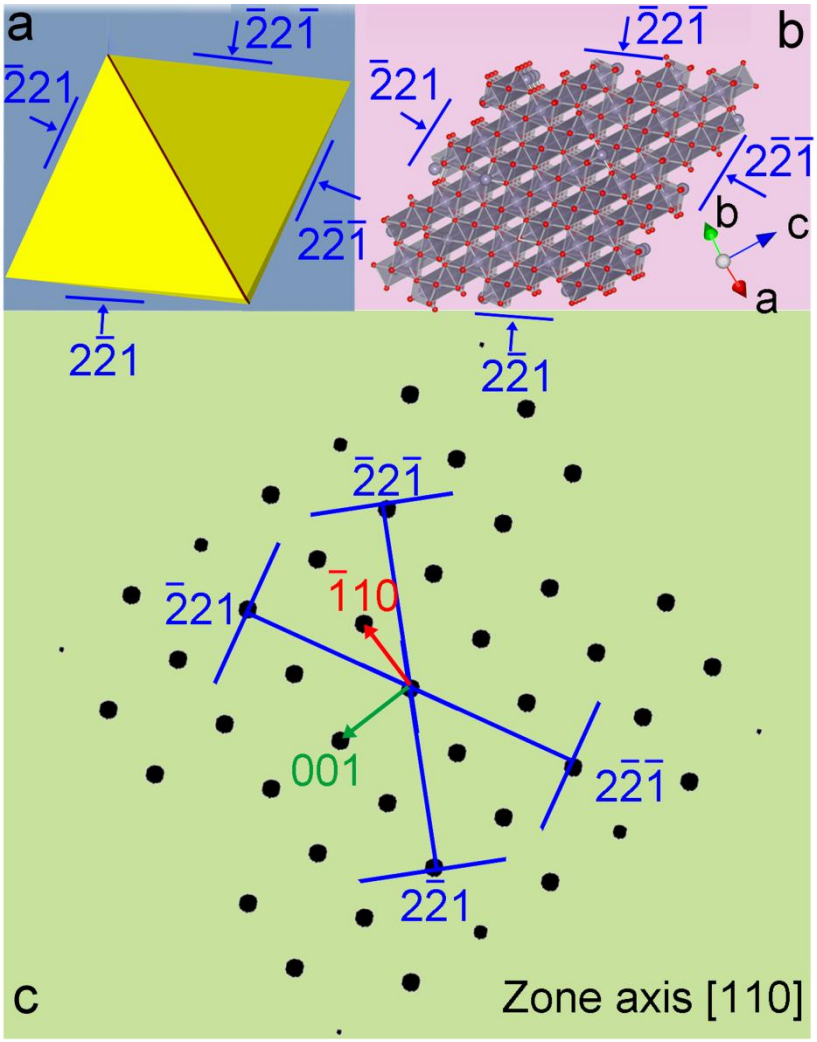

Figure S2. Schematic illustration of octahedral SnO_2 nanocrystals viewed along the [110] direction. (a) The geometric model, (b) The simulated crystal structure, and (c) The simulated electron diffraction pattern along the [110] zone axis. The relationship between the rhombic outline and the crystal planes along the [110] direction can be identified and the pyramid planes can be indexed as the {221} facet.

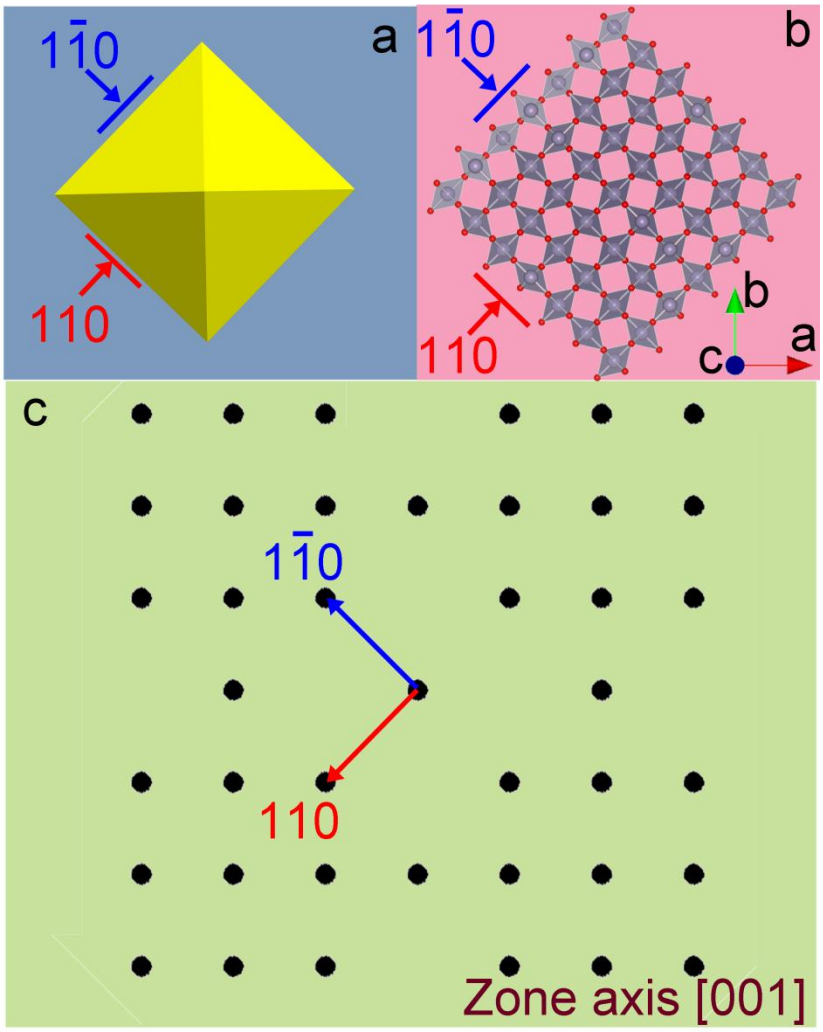

Figure S3. Schematic illustration of the octahedral SnO_2 nanocrystal viewed along the [001] direction. (a) The geometric model, (b) The simulated crystal structure and (c) The simulated electron diffraction pattern along the [001] zone axis. The relationship between the squared outline and the crystal planes along the [001] direction can be identified.

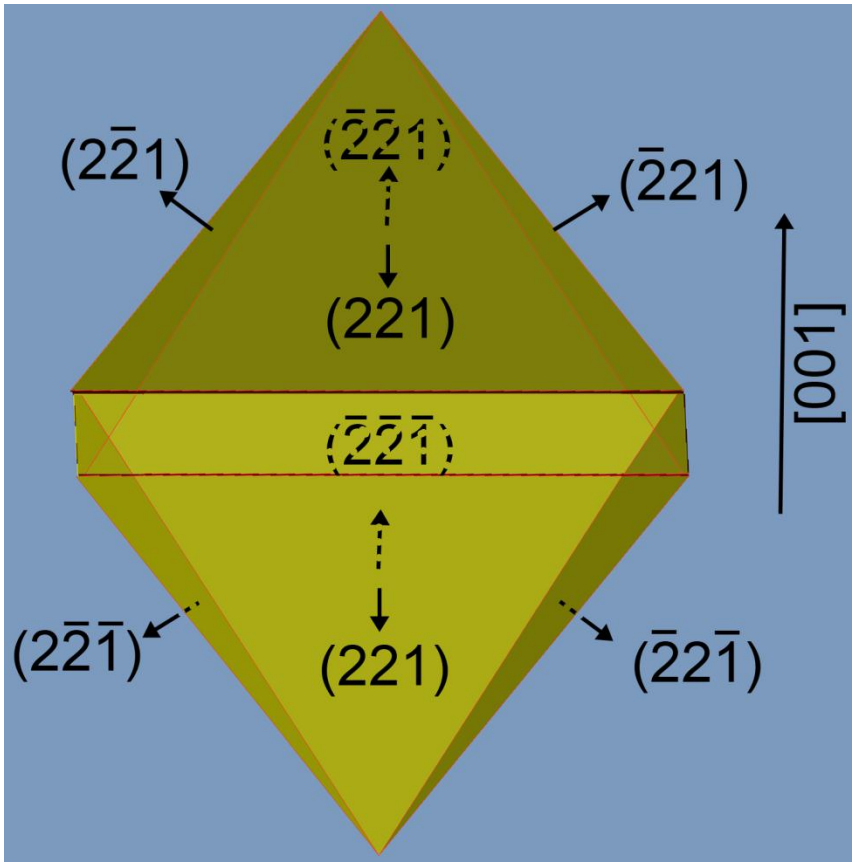

Figure S4. The geometric model of the as-prepared octahedral SnO_2 nanocrystals, in which different facets and the growth direction have been labelled.

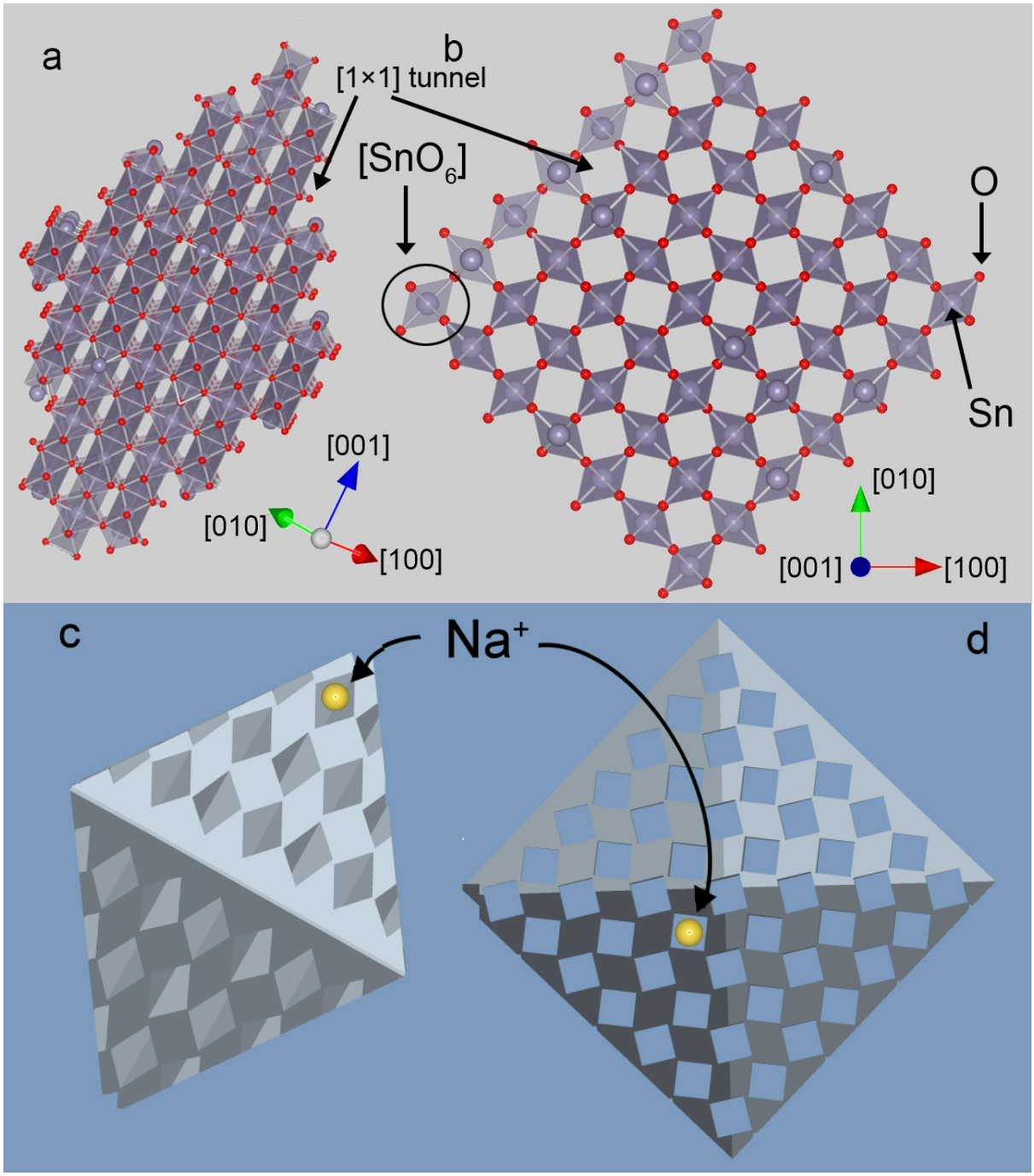

Figure S5. The crystal structure of octahedral SnO_2 nanocrystals viewed from the [110] (a) and [001] (b) directions. The Sn^{4+} and O^{2-} ions, coloured in grey and red, respectively. From (b), we can directly observe the 2 × (1 × 1) tunnels composed of individual chains of the SnO_6 octahedral units. (c) and (d) are their geometric models, corresponding to (a) and (b), respectively.

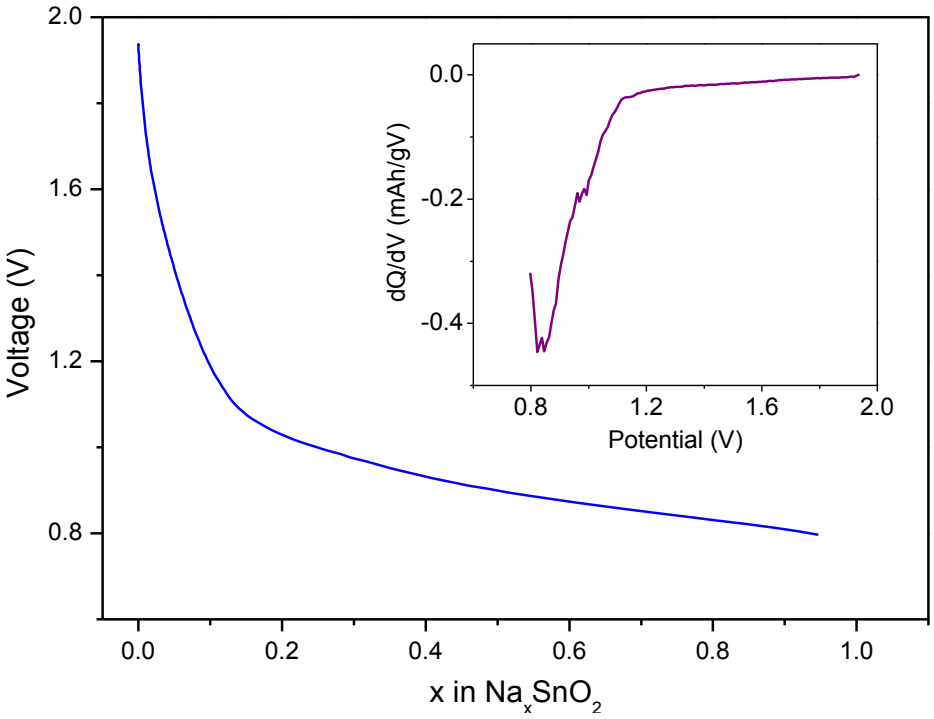

Figure S6. The discharge profile of SnO_2 nanocrystal electrode, which was discharged to 0.8 V. The inset is the corresponding differential discharge capacity versus voltage.

Synthesis of the nanometre-sized SnO_2 particles

The nanometre-sized SnO_2 particles were synthesized by a hydrothermal method. In a typical synthesis process, 9 ml 6 M NaOH (Sigma-Aldrich, ≥ 99%) solution was added into 10 ml 2 M $SnCl_2 \cdot 5H_2O$ (Sigma-Aldrich, ≥ 98%) solution under vigorous stirring. The mixture was then transferred into a Teflon lined autoclave (25 ml in capacity) and heated at 180 °C for 12 hours in an air-flow electric oven. After cooling down to room temperature, the black product was collected by centrifugation and washed thoroughly with de-ionised water for several times. After drying at 60 °C in vacuum oven overnight, the products were further sintered in tube furnace at 500 °C for 5 hours.

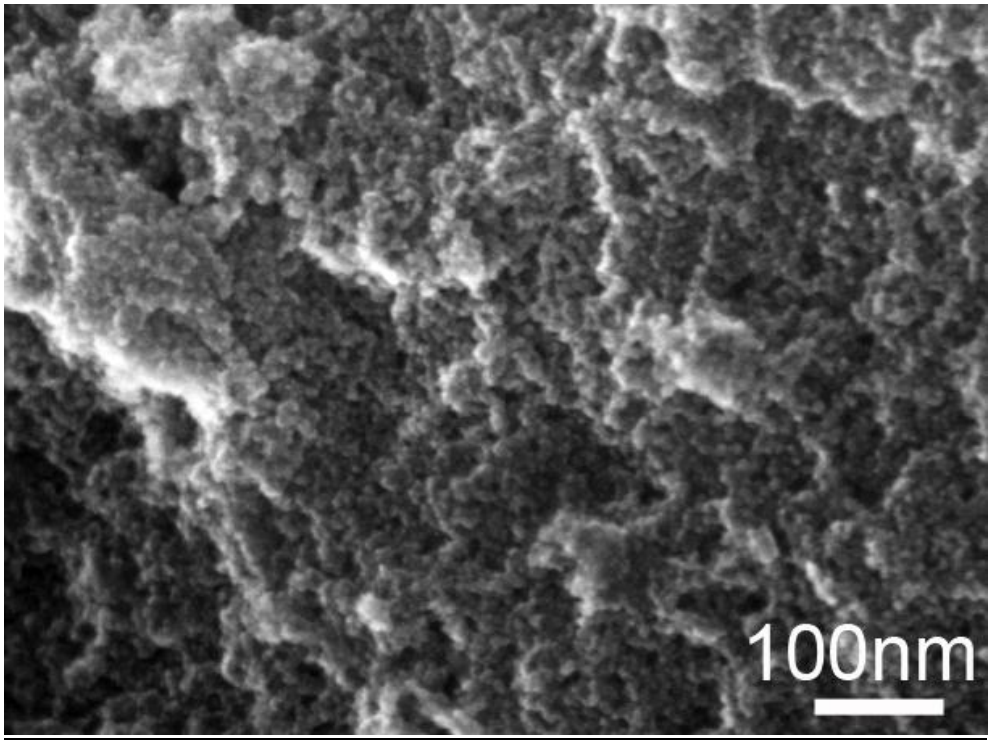

Figure S7. SEM of nanometre-sized SnO_2 particles

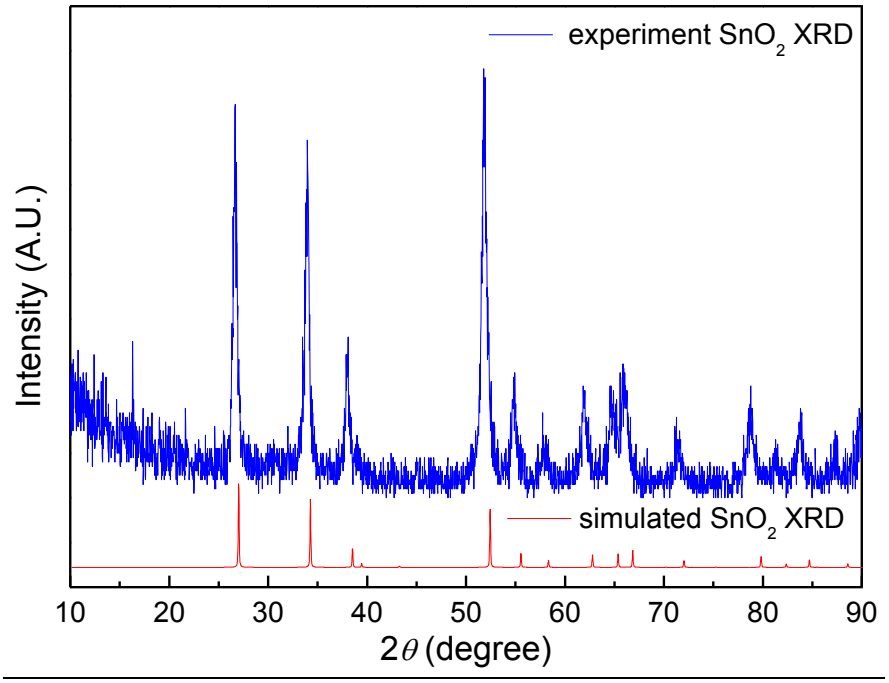

Figure S8. XRD pattern of nanometre-sized SnO_2 particles

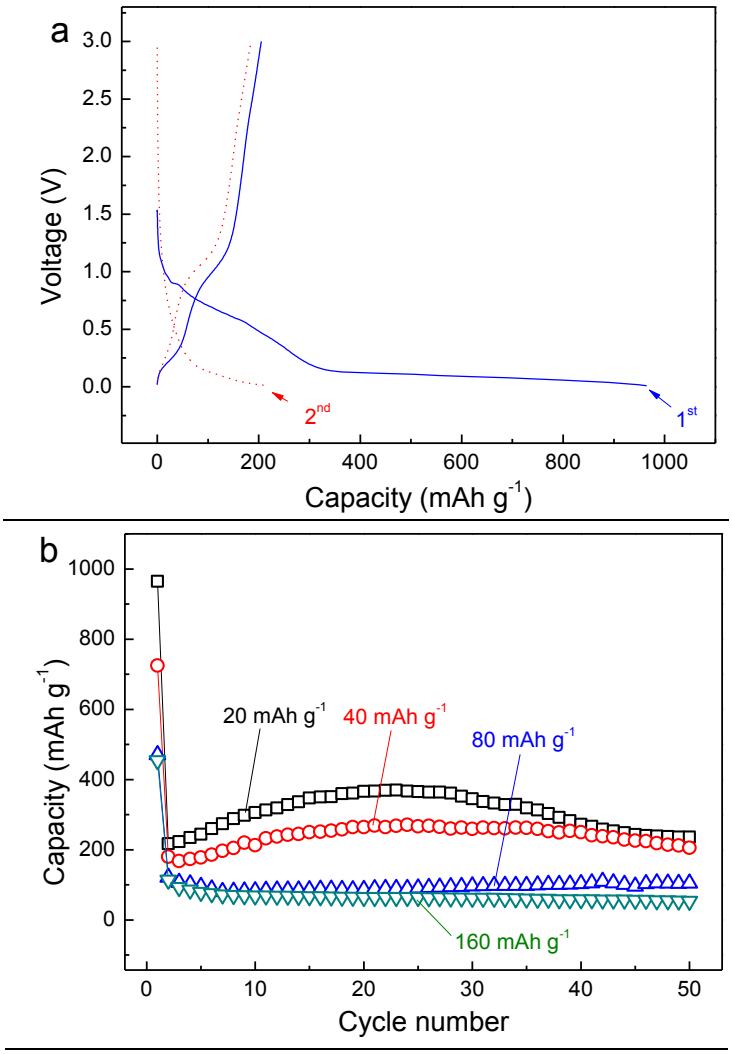

Figure S9. (a) Discharge and charge profiles of nanometre-sized SnO_2 in the 1st and 2nd cycles. (b) Discharge capacity *vs.* cycle number of nanometre-sized SnO_2 at current densities of 20, 40, 80, and 160 mA g^{-1}.

Table S1. d-Spacing & Miller Indices of SnO_2, Sn, Na_2O and Na_9Sn_4.

SnO_2 (71-0652)		Sn (87-0794)		Na_2O (77-2148)		Na_9Sn_4 (31-1326)	
d-spacing	h k l	d-spacing	h k l	d-spacing	h k l	d-spacing	h k l
3.3502	1 1 0	3.74643	1 1 1	3.2049	1 1 1	3.6791	115
3.1866	0 0 1	2.2942	2 2 0	2.775	2 0 0	3.4021	026
2.3692	2 0 0	1.9565	3 1 1	1.9622	2 2 0	2.9620	0010
2.1189	2 1 0	1.8732	2 2 2	1.6733	3 1 1	2.9073	028
1.7644	2 1 1	1.6223	4 0 0	1.3875	4 0 0	2.5453	134
1.6751	2 2 0	1.4887	3 3 1	1.2732	3 3 1	2.3756	206
1.5933	0 0 2	1.3246	4 2 2	1.2410	4 2 0	2.1870	138
1.4983	3 1 0	1.2488	5 1 1	1.1329	4 2 2	2.1200	046